JOURNAL OF CATALYSIS 152, 243–251 (1995)

Crystallite Shape and Iron Lattice Orientation in the Ammonia Synthesis Catalyst

Børge Holme[1] and Johan Taftø

Department of Physics, University of Oslo, P.O. Box 1048 Blindern, N-0316 Oslo, Norway

Received November 2, 1993; revised October 3, 1994

The morphology of reduced and stabilized ammonia synthesis catalyst, which is produced by reduction of magnetite, has been studied using optical microscopy with polarized light and transmission electron microscopy. The combined use of these techniques has revealed micrometer size regions of different pore structure within the reduced magnetite grains. One of these structures consisting of parallel sheets of bcc-iron is described. Both the sheets and the space between them are of typical thickness, 15 nm. The orientation of iron in the sheets is related to the former magnetite crystal lattice by a rotation of 45° about one of the three ⟨100⟩ axes. This ⟨100⟩ axis, common to both magnetite and iron, is normal to the iron sheets. The sheet-like iron regions display large scale magnetic domains with in-plane magnetization within the sheets.

INTRODUCTION

The ammonia synthesis catalyst is made by reduction of magnetite, Fe_3O_4, containing about 2% promoters, typically oxides of aluminum, potassium, and calcium. During reduction, oxygen is removed by hydrogen gas. Porous, body-centered cubic iron (bcc-iron or α-Fe) and promoter oxides are left behind.

Because of its great importance, the ammonia synthesis catalyst has been studied extensively during the past decades. Several models of the catalyst morphology have been proposed; see Ref. (1) for a review. In a recent article (2), Schlögl described the catalyst as consisting of blocks of iron in a network of pores, the iron blocks being separated by spacers of segregated promoter oxides. Each block of iron had an internal structure where platelets of single crystal iron were loosely stacked and the normal to the iron platelets was the ⟨111⟩ direction.

Pennock *et al.* (3) investigated the structure of the unreduced and reduced catalyst and performed *in situ* reduction of magnetite in a transmission electron microscope (TEM). They observed iron crystallites and pores of approximately 20–30 nm size and suggested that the pores grew along {111} planes in the magnetite. In some regions all the iron crystallites were found to have the same crystallographic orientation. This was thought to result from epitaxial nucleation of iron on magnetite during reduction since the orientation relationship was found to be the well-established epitaxy relation between α-Fe and magnetite (4). This epitaxy is such that the {100} planes of iron and magnetite are parallel. The ⟨010⟩ and ⟨001⟩ directions of iron are parallel to the ⟨011⟩ and ⟨0$\bar{1}$1⟩ directions of magnetite.

Based on a TEM study Taftø *et al.* (5) reported the presence of three different iron orientations within the same reduced magnetite grain. This was attributed to a Bain-like transformation from the magnetite to body-centered cubic iron. The three iron orientations were equivalent and were shown to follow from the iron-magnetite epitaxy and the cubic symmetry of magnetite. From dark field images it was established that regions containing one crystallographic orientation of iron could extend for more than 10 μm. Such regions where described as "porous single crystals of α-Fe."

The present work is part of a comprehensive investigation of stabilized ammonia synthesis catalysts. In order to study the morphology and microstructure of the catalyst over a broad range of magnifications, optical microscopy, transmission electron microscopy, and electron diffraction were used. The primary motivation for this study is to obtain a better understanding of the reduction process when promoted magnetite is converted into porous iron.

In this paper we show that the porous single crystals of α-Fe have a distinct sheet-like pore structure with a well-defined orientation relative to the original magnetite. We further confirm the observations of Refs. (3) and (5) regarding the crystallographic orientations of iron for this particular structure. Finally, the magnetic properties of these regions are briefly discussed.

EXPERIMENTAL

The specimens used in the present study were industrial Norsk Hydro unreduced AS-4 and prereduced AS-4-F

[1] To whom correspondence should be addressed.

0021-9517/95 $6.00

ammonia synthesis catalysts made from Al-, Ca-, and K-promoted magnetite particles of size 6–10 mm. In addition, catalyst particles that had been used in an ammonia synthesis reactor for 5 years were studied by optical microscopy.

Some unreduced catalyst particles were reduced under laboratory conditions, often only two or three particles at a time. During these reductions, the temperature was typically raised from 690 to 800 K (417–527°C) at an average rate of 1 K/h. The reduction gas was pure hydrogen at atmospheric pressure. In some cases we intentionally reduced the catalyst particles to 80% of total possible weight loss. In these particles, a core of unreduced magnetite was left at the center of some former magnetite grains, in accordance with the "crackling core" model described in Ref. (6).

During reduction, there is no change in the outer shape of the catalyst particles, whereas the volume of solid matter is halved. This means that the reduced magnetite consists of porous iron with half the apparent volume being pores.

The reduced specimens were stabilized to prevent spontaneous combustion in air. Oxygen was slowly added to the reduction chamber until the oxygen partial pressure of air was reached. The downstream gas temperature measured 1 cm after the samples did not exceed 300 K during this process, which typically lasted for 30 to 60 h. In stabilized samples the iron surface is covered with 1.5–3 nm of oxide (7), enough to prevent further oxidation in air at room temperature. The reduced catalyst particles were moulded in epoxy resin and later ground and polished according to standard metallographic techniques.

Specimens selected for TEM examination were cut into slices, ground and polished to about 100 μm thickness, and subsequently etched in a Gatan ion mill model 600. The ion beam made an angle of 12° relative to the plane of the specimen. The gun voltage was 4 kV and the gun current about 1 mA.

The optical microscope used in this study was a Reichert–Jung MeF 3 metallography microscope equipped with a complete set of filters for polarization microscopy. The images were obtained using crossed polarizer and analyzer, and a 273 nm retarder plate that was traversed twice by the light. The angle between the transmission axis of the analyzer and the fast axis of the retarder was 6°.

By suspending the specimens under a glass plate in a magnetic field, the TEM specimens could be examined in the optical microscope after ion thinning. This proved very useful in establishing the connection between observations in the optical microscope and the small scale details revealed by TEM. It became routine to photograph a TEM specimen in the optical microscope before studying it in TEM. The catalyst is known to be very inhomogeneous containing reduced and unreduced iron/promoter oxide phases in addition to reduced wüstite and magnetite. In order to identify the different phases, we compared optical micrographs with TEM images and diffraction patterns. In the case of magnetite and wüstite, these phases can be distinguished by their different morphology; see micrographs in Ref. (8).

The transmission electron microscope was a JEOL 200 CX operated at 200 kV accelerator voltage.

Some noticeable magnetic properties of the catalyst were discovered by applying magnetic particles to the surface of optical microscope specimens. The most convincing results were obtained using a mixture of paramagnetic and nonmagnetic microspheres in a solution of water and a surfactant that prevented agglomeration of the spheres. A few drops of the suspension were applied to the polished surface using a pipette dropper. Waiting a couple of minutes allowed the particles to settle down on the surface. Subsequent washing under running water and drying in a stream of hot air removed all spheres that were not firmly attached to the specimen. The sample was studied in the optical microscope where the 3-μm spheres could easily be resolved. Magnetic and nonmagnetic spheres appeared in different colors. Very few of the nonmagnetic spheres adhered to the surface in any of the experiments, indicating that the paramagnetic spheres were held in place by magnetic forces.

FIG. 1. Reduced magnetite grain in the ammonia synthesis catalyst. This optical micrograph is made using polarized light and a gypsum filter in order to create colors that highlight the areas under investigation. The letters x, y, and z show examples of these three kinds of areas. The colors are not an intrinsic property of the regions. A 90° rotation of the microscope specimen stage makes the yellow regions (x) turn blue and blue areas (y) turn yellow, making the cracks in y-type regions clearly visible. Brown regions (z) remain brown.

FIG. 2. The thin edge of a TEM specimen made from an industrially reduced catalyst particle is photographed in the optical microscope (a) and in the bright field mode in TEM (b). The area in (b) corresponds to the box in (a) and shows that the yellow, brown, and blue colors of the optical micrograph are associated with regions of sheet-like pore structure with a particular pore orientation.

FIG. 5. Detection of magnetism in the polished surface of an industrially reduced catalyst specimen. Micrograph (a) shows a part of the catalyst where some of the reduced magnetite grains display yellow and blue colors in certain regions. The same area is shown in (b) after magnetic microspheres were applied to the surface. The spheres seem to collect on the bright regions of image (a). No spheres adhere to the smooth, light-brown regions of the type indicated by the tip of the arrow. This is consistent with the assumption of in-plane magnetization within the iron sheets.

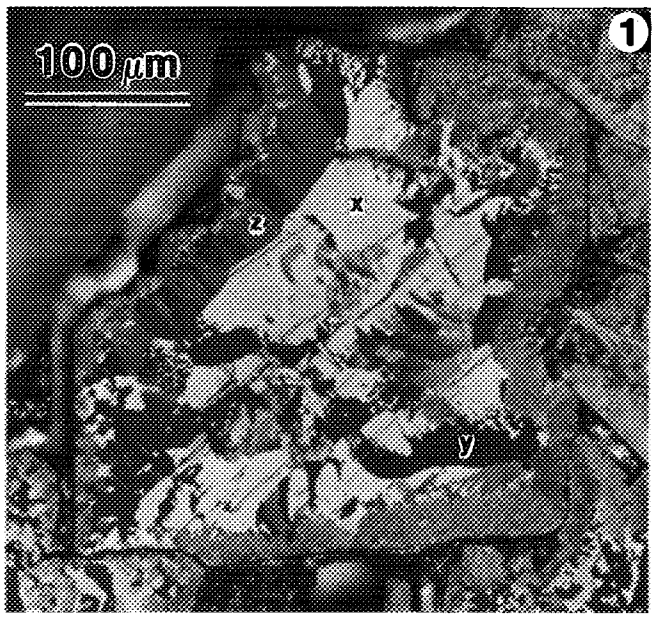
100 μm
1
z
x
y

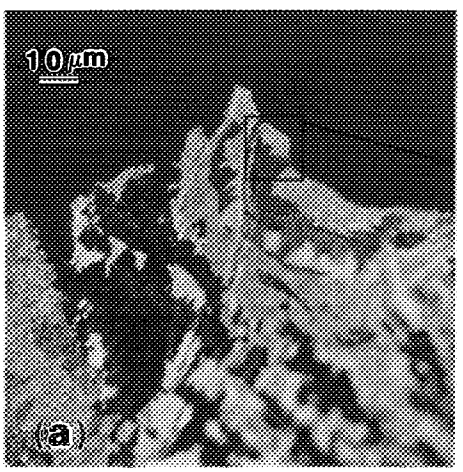
10 μm
(a)

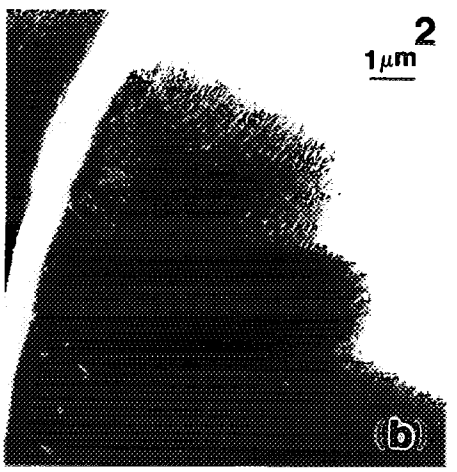
1 μm 2
(b)

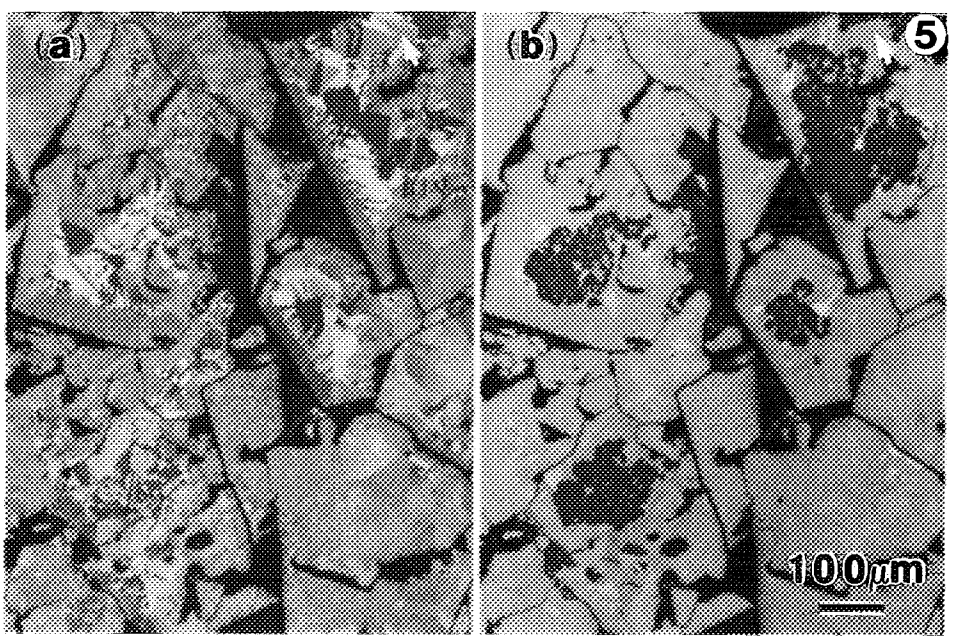
(a)
(b)
5
100 μm

RESULTS AND DISCUSSION

Figure 1 is an optical micrograph of an industrially reduced and stabilized catalyst showing a particularly bright part of the polished surface. The image was obtained in the polarization contrast mode. Yellow (x), blue (y), and brown (z) regions of porous iron are visible inside a reduced magnetite grain. The grain has an approximately square outline. In the yellow regions, several dark and parallel cracks are seen. A similar set of cracks, normal to the first, is present in the blue areas but the cracks are hard to reproduce in this image due to the dark background. The difference in color between yellow and blue regions is a result of the use of polarized light. The symmetry equivalence of regions x and y was apparent after a 90° rotation of the specimen when their colors were interchanged and the cracks in y could easily be seen. In the dark-brown regions at the upper left, no cracks are observed. This is consistent with the assumption that the cracks lie along three mutually perpendicular planes, like the faces of a cube. The cracks in the brown regions are thus expected to lie parallel to the image plane and do not intersect it. Sectioning experiments where the surface was repeatedly polished and observed in the optical microscope confirmed that the cracks in yellow, blue, and brown regions are approximately planar and mutually perpendicular. Further, from TEM examination of partly reduced samples it was found that a spinel phase is present in the reduced regions and that this phase has the same crystallographic orientation as the original magnetite in the interior of the grain. This makes it possible to correlate the orientation of cracks and pores observed on TEM samples with the original magnetite cube axes. It was found that the plane-shaped cracks are normal to the cube axes of the original magnetite crystal. This is consistent with the crack directions of Fig. 1. Magnetite prefers to crystallize as regular octahedra (9), thus displaying the {111} planes at the outer faces. If a perfect octahedral magnetite crystal is cut such that the new face has a square outline, the cut will have been made normal to one of the cube axes of magnetite, and the other two cube axes will be along the diagonals of the square (see Fig. 6a which shows this geometry). Disregarding the broken corner of the grain in Fig. 1, the cracks are also along the square diagonals and thus normal to a presumed cube axis.

Figure 2 shows a TEM specimen as viewed in the optical microscope (Fig. 2a) and in the bright field mode of the transmission electron microscope (Fig. 2b). There seems to be a one-to-one correspondence between the pore structure of the specimen and the colors that appear in the optical microscope. For instance, in the yellow regions of Fig. 2a, the pores are predominantly in a direction from the lower-left to the upper-right corner as is clearly seen in the bright field image, Fig. 2b. If the specimen is rotated by 90° in the optical microscope, the yellow regions turn blue and vice versa while the brown areas remain brown. Such color effects are known to occur when the specimen surface is optically anisotropic, e.g., if the crystal under study has lower than cubic symmetry or if there is a distinct surface relief (10). Similar color effects as observed here are visible on anodized aluminum, but in that case an oxide layer of more than 500 nm must be grown on the aluminum surface. This is more than a hundred times thicker than the oxide layers on the catalyst surface. Further, an oxide layer with lower than cubic crystal symmetry is required in order to have optical anisotropy. The cubic oxides of iron will not give this effect and this is confirmed by observations of unreduced magnetite grains which appear evenly brownish regardless of orientation. In the case of the reduced catalyst, it thus seems reasonable to assume that the relief produced by the pores in the specimen surface is the cause of the optical anisotropy.

The sheet-like iron regions were observed in all classes of reduced samples, although in differing amounts. Differences between individual particles were much greater than differences resulting from dissimilar reduction conditions. There are, however, indications from optical microscopy and TEM that the pore structure of the iron sheets is most distinct in the laboratory reduced samples, slightly less distinct in the industrially reduced particles and more blurred in the samples that had been used in a synthesis reactor for five years; compare Figs. 2 and 3. These small differences suggest that the iron sheets are stable enough to remain largely unchanged for extended periods under ammonia synthesis conditions.

The pore structure of a laboratory reduced sample is examined more closely in Fig. 3. The TEM bright field image in Fig. 3a shows two kinds of regions with a distinct horizontal and vertical pore orientation. Here, the iron sheets are viewed "edge on" in both regions, as shown schematically in the lower part of Fig. 3a where two sets of square slabs are stacked together to form two adjacent "porous cubes" and the slabs are seen edge on. If the porous cubes were rotated 25° about a horizontal axis, they would appear as in the drawing in Fig. 3b. The vertical slabs are still seen edge on, whereas the horizontal slabs overlap. A similar effect was observed when the TEM specimen was tilted 25°, as determined from diffraction patterns, and the bright field image is shown in Fig. 3b. The vertical pores are still clearly visible, while the horizontal pore structure is less distinct. Compare for instance the region of horizontal pores above the scale bar in Fig. 3b with the same region in Fig. 3a, and notice the sharper white openings in Fig. 3a.

The iron sheets are seen to be about 10–20 nm thick with the pores between them of approximately the same dimensions. Although the sheet-like regions described

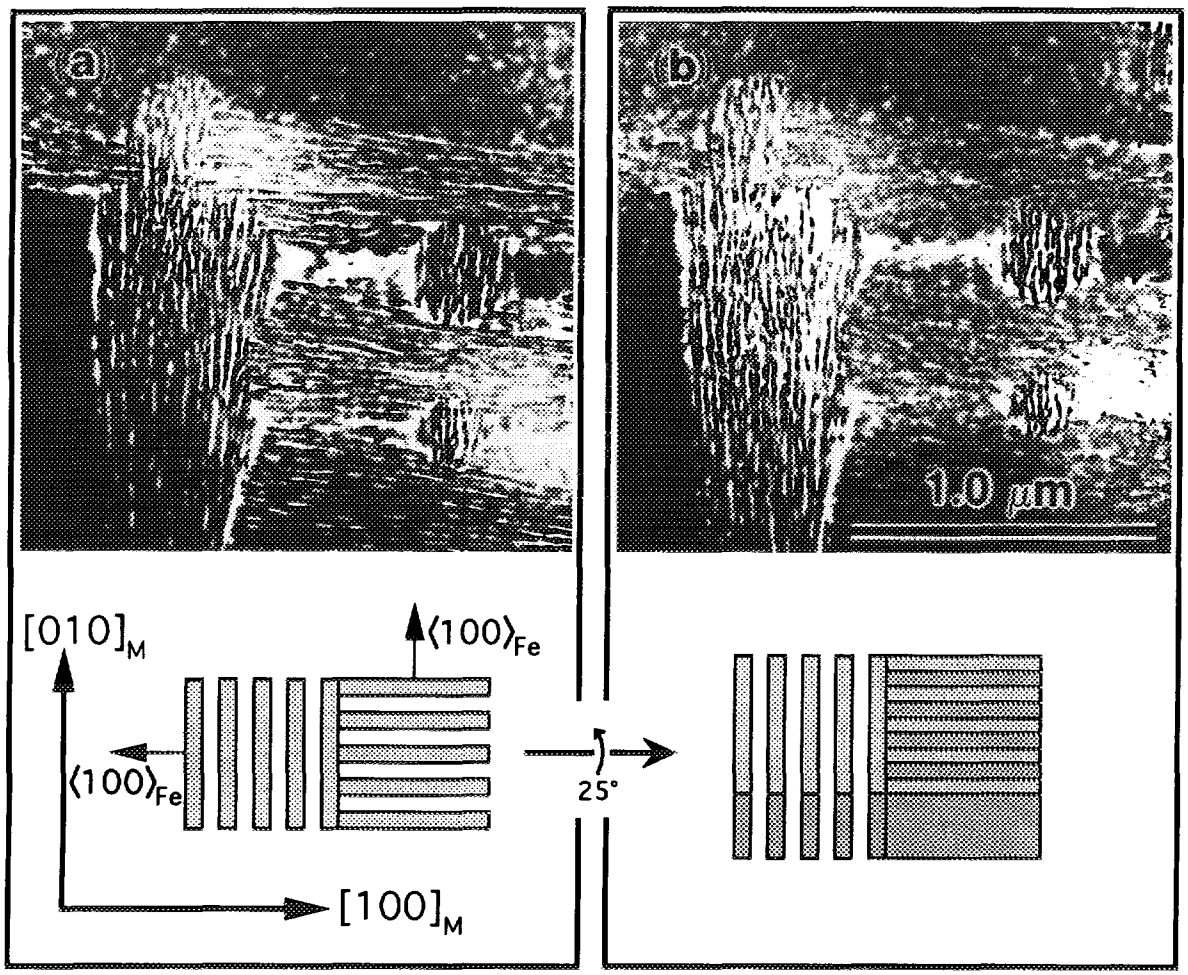

FIG. 3. Bright field images from a laboratory reduced sample and drawings showing the geometry of iron sheets in the catalyst. From image (a) to (b) the specimen was tilted 25°, thus blurring the horizontal pores. The directions indicated by arrows show crystallographic relations between iron in the sheets and the original magnetite from which the catalyst was made.

here are present in rather small quantities within reduced magnetite grains, it is interesting to note that a pore structure with a sheet thickness b = 15 nm would lead to a specific iron surface area of $2/b\rho$ = 17 m^2/g. Here ρ = 7.9×10^3 kg/m^3 is the mass density of iron. The measured surface area of the ammonia synthesis catalyst is typically in the range 10–20 m^2/g (2, 11).

Examination of specimens in a scanning electron microscope showed that the catalyst contains parallel cracks of width ranging from 15 nm to about 2 μm. The larger cracks are also seen in the optical microscope, Figs. 1 and 2a. These cracks are parallel to the iron sheets and may result from a partial collapse of the pore structure. Regions with parallel sheets frequently extend for several tens of micrometers. It seems likely that this open sheet structure might collapse during reduction, forming large lens-shaped cracks and a somewhat denser stacking of the iron sheets on each side, thus reaching a relatively stable state.

The remaining regions in Figs. 3a and 3b are areas where the iron sheets are parallel to the image plane and no particular pore structure is observed.

The coordinate system and arrows in the drawing of Fig. 3a show the various orientation relations of the iron sheets. First, the sheets are parallel to {100} planes in the original magnetite crystal structure. Secondly, the orientation of the iron unit cell in the single crystal sheets of iron is such that a ⟨100⟩ direction of iron is normal to the sheets, suggesting that, on the average, the iron sheets expose the {100} crystal surface.

Our results are based on the study of several specimens, all showing regions containing the described pore structure. The orientation relations are deduced from diffraction and dark field images as shown in Fig. 4.

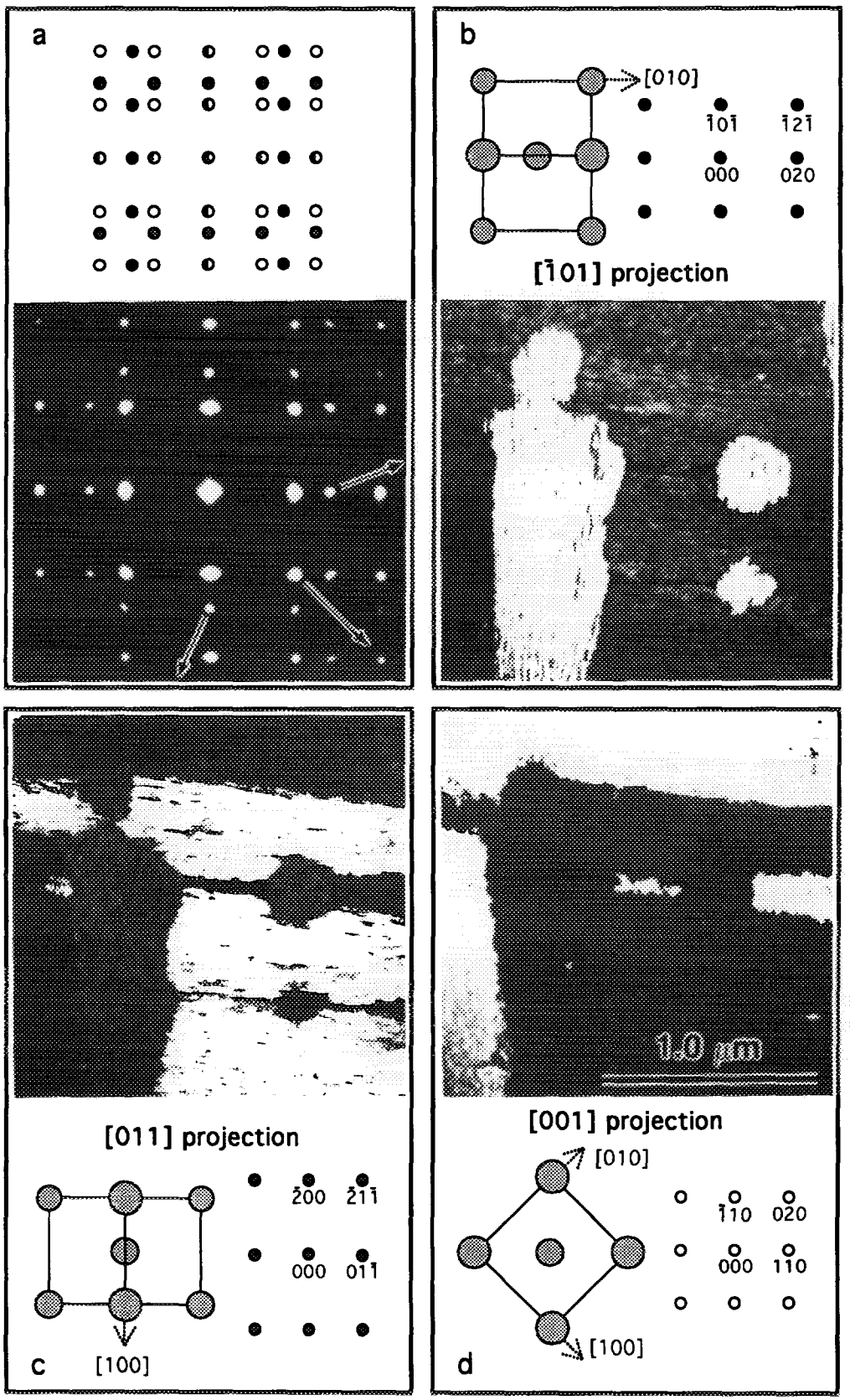
a
b
[010]
$\bar{1}01$
$\bar{1}2\bar{1}$
000
020
[$\bar{1}$01] projection
1.0 μm
[011] projection
$\bar{2}00$
$\bar{2}1\bar{1}$
000
01$\bar{1}$
c
[100]
[001] projection
[010]
$\bar{1}10$
020
000
110
[100]
d

The diffraction pattern in Fig. 4a is interpreted as a compound pattern from three crystallographically equivalent variants of body-centered cubic iron and a ⟨001⟩ projection from magnetite. The drawings in Figs. 4b, 4c, and 4d show the orientation of the iron unit cells and the corresponding diffraction pattern if the incident electron beam is normal to the paper. By superimposing the three patterns, the pattern in Fig. 4a is generated. It is thus established that the illuminated area contains iron of these three orientations. The dark field images in Figs. 4b, 4c, and 4d are obtained from the kinds of reflections indicated by arrows in Fig. 4a and show where the iron of different orientation is located. These images are from the same area as Fig. 3, and it is obvious that parallel sheets contain iron of the same crystallographic orientation. In Fig. 4d those regions light up where the sheets are parallel to the image plane.

Four weak inner spots, halfway between the 000- and 020-type reflections in Fig. 4d, were visible on the TEM negatives. These are the 220-type reflections from magnetite or a similar spinel phase enriched in aluminum. As mentioned above, this phase has been found to have the same crystallographic orientation as the original magnetite. During the reduction to α-Fe, the less reducible aluminum ions, originally dissolved in the magnetite, remain in aluminum-enriched spinel phases (12). The crystallographic relationship with the original magnetite is conserved in this process. The situation is further complicated in the study of *stabilized* specimens where the uncovered regions of the iron surfaces have been reoxidized. One would thus expect to have both aluminum-enriched $Fe_{3-x}Al_xO_4$ from the reduction and more pure Fe_3O_4 from the stabilization present in the specimens. By accurate lattice parameter measurements it should be possible to distinguish these phases, which would have rather similar lattice spacings.

Comparing the dark field images and the orientation of the corresponding unit cells of iron we conclude that the local pore and crystallographic structure is the same in each of the three regions; parallel sheets of α-iron, about 15 nm thick and with a ⟨100⟩ axis of iron normal to the sheets. The iron variants are equivalent and can be viewed as a result of the cubic symmetry of the original magnetite as well as the epitaxial lattice matching. The unit cell dimension of magnetite, $a = 0.840$ nm, is such that $\sqrt{2}a/4 = 0.297$ nm which deviates from the α-iron cell dimension 0.287 nm by 3.5%. Thus, the magnetite and α-iron structures match quite well when the unit cell of iron is rotated 45° about a common cube axis.

A recent scanning tunneling microscopy (STM) study (13) shows indications of ridges in the catalyst surface along the ⟨011⟩ direction of iron. Our ⟨100⟩ sheet normal is perpendicular to the ⟨011⟩ direction. Thus these observations do not contradict our findings. However, due to the large number of structures in this catalyst, agreement between different studies may be accidental.

Detection of surface magnetism is shown in Fig. 5. The two micrographs in Figs. 5a and 5b are made from exactly the same area. Figure 5a shows a part of the catalyst with several grains containing regions of blue and yellow colors and dark cracks. These are the kind of regions examined in the present study. The micrograph in Fig. 5b was made with the polarizing filters 10° out of crossed position in order to fade the colors and highlight the clusters of brown-red magnetic microspheres. It is apparent from the two images that the magnetic spheres stick to regions which in the polarization contrast mode of Fig. 5a show up in bright colors. Repeated experiments on this and other specimens show similar clustering, although not always as distinct as in Fig. 5.

The grain at the upper right corner in Fig. 5a has a few featureless brown regions. One of these is at the tip of the white arrow. Both the color and the grain geometry indicate that here the iron sheets are parallel to the polished surface, as in the region marked z in Fig. 1. It is worth noting that no spheres seem to collect on the corresponding regions in Fig. 5b.

Both theoretical and experimental work on thin Fe(100) films indicate that for sheet thicknesses of 10–20 nm, the magnetic moment will be within the plane of the sheet (14–16). The simplest model for the magnetization would be that all magnetic moments were parallel in all sheets within one porous iron region. In this model, each yellow and blue region of Fig. 5a would be a "porous single domain."

Assuming that grinding and polishing the specimen does not change the magnetic domain structure, the proposed model should generally result in relatively large leakage fields out of yellow and blue regions. The magnetic microspheres should adhere to the polished surface in these regions. They should not collect on areas where the magnetization is parallel to the surface, e.g., in the featureless brown regions mentioned above.

The simple domain structure model suggested here

FIG. 4. Diffraction and dark field images from the same region as in Fig. 3. The iron diffraction patterns in (a) are made up of three individual patterns that are drawn separately in (b), (c), and (d). The drawings of iron unit cells show the orientation of iron that gives rise to each pattern. Arrows indicate the kind of reflections used in the three dark field images. White areas in the dark field micrographs show where iron of the three crystallographic orientations is located. Note that a ⟨100⟩ axis of iron is normal to all the sheets.

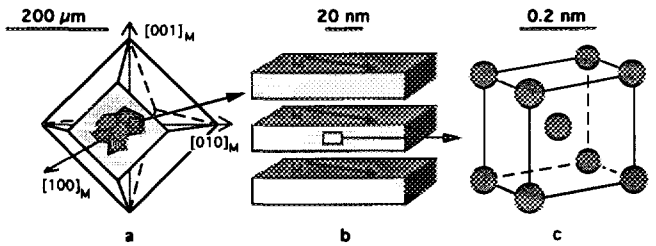

FIG. 6. Three schematic drawings summarize the structure of the sheetlike iron regions described in this paper. Hatched areas in (a) represent the three kinds of regions with sheet-like pore structure seen within an octahedral magnetite grain. The three regions differ in their pore orientation relative to the original magnetite. These regions of irregular shape extend for up to 50 μm. Each region consists of sheet-like iron crystals stacked parallel to each other, (b). The regions show large-scale ferromagnetic order with in-plane magnetization as indicated by the arrows. Within parallel sheets, the crystallographic orientation of iron is the same and a ⟨100⟩ direction is normal to the sheets as shown in (c).

for the sheet-like iron regions is consistent with the experiment of Fig. 5. However, a full description of the magnetic domain structure for the entire volume of the iron catalyst will surely be much more complex.

In catalyst particles from the 6–10 mm size fraction, the bright regions associated with the structure described here are most often observed in the outer 2 mm of the particle. It is interesting to note that during ammonia synthesis it is mainly the outer 1–2 mm surface layer of the catalyst particle that participates in the reaction (11), a consequence of slow diffusion inside the particle. Thus, despite their low *total* volume fraction, the regions with sheet-like morphology described here may represent a relatively large part of the volume where catalysis takes place. Moreover, it is known from single crystal experiments (17) that the clean Fe(100) surface is generally about one-sixth as active as the most active plane, Fe(111). However, according to Ref. (18), potassium eliminates the difference between the activity of Fe(100) and Fe(111) in dissociative nitrogen chemisorption, which is the rate-limiting step in ammonia synthesis. It has also been reported that pretreatment with water vapor or ammonia of clean and promoter-oxide-covered iron surfaces may increase the catalytic activity of the Fe(100) face by causing small scale surface restructuring into facets of the more active Fe(111) plane (13, 19–21). Thus, both promoter effects and restructuring may contribute to give the ⟨100⟩ iron sheets a higher catalytic activity. However, other experiments are required in order to determine the specific catalytic activity of the sheet-like iron regions.

Studies of a large number of specimens have revealed that at least three other types of pore structures with many more iron orientations are present in the catalyst. The sheet-like iron regions described here occupy typically 0–20% of a catalyst particle. The majority of reduced magnetite grains appear plain or somewhat mottled as in some regions of Fig. 5a. The large variety of structures should be taken into account when comparing results from the literature since various investigators may have examined *different* structures within similar catalyst specimens.

In conclusion, examination of the ammonia synthesis catalyst using different microscopic techniques has yielded new experimental results that may help elucidate the transformation from magnetite to porous iron during reduction. We have in this paper described *one* of the structures observed in the catalyst. The results are summarized in Fig. 6 on length scales from tenths of millimeters down to Ångströms.

ACKNOWLEDGMENTS

The authors thank Norsk Hydro A/S for active support, in particular the Hydro Agri Catalyst Department for providing specimens and the Research Center for performing reduction experiments. This project was sponsored by the Norwegian Research Council (Norges forskningsråd) and this contribution is gratefully acknowledged.

REFERENCES

1. Borghard, W. S., and Boudart, M., *J. Catal.* **80,** 194 (1983).
2. Schlögl, R. *in* "Catalytic Ammonia Synthesis" (J. R. Jennings, Ed.), p. 19. Plenum, New York, 1991.
3. Pennock, G. M., Flower, H. M., and Andrew, S. P. S., *J. Catal.* **103,** 1 (1987).
4. Mehl, R. F., McCandless, E. L., and Rhines, F. N. *Nature,* **134,** 1009 (1934); Mehl, R. F., and McCandless, E. L., *Nature,* **137,** 702 (1936).
5. Taftø, J., Kristiansen, L. A., and Fuglerud, T., *Philos. Mag. Lett.* **64,** 105 (1991).
6. Park, J. Y., and Levenspiel, O., *Chem. Eng. Sci.* **30,** 1207 (1975).
7. Menon, P. G., and Skaugset, P., *Appl. Catal. A* **115,** 295 (1994).
8. Clausen, B. S., Mørup, S., Topsøe, H., Candia, R., Jensen, E. J., Baranski, A., and Pattek, A., *J. Phys. Colloq.* **C6,** 245, (1976); Jensen, E. J., Topsøe, H., Sørensen, O., Krag, F., Candia, R., Clausen, B. S., and Mørup, S., *Scand. J. Metall.* **6,** 6 (1977).
9. Hurlbut Jr, C. S., and Klein, C., "Manual of mineralogy," 19th ed. Wiley, New York, 1977.
10. Craig, J. R., and Vaughan, D. J., "Ore microscopy and ore petrography," Wiley, New York, 1981.
11. Bakemeier, H., Huberich, T., Krabetz, R., Liebe, W., Schunck, M., and Mayer, D., *in* "Ullmann's Encyclopedia of Industrial Chemistry" (W. Gerhartz, Ed.), Vol. 2A, p. 143. VCH Verlagsgesellschaft, Weinheim, Germany, 1985.
12. Peters, C., Schäfer, K., and Krabetz, R., *Z. Elektrochem.* **64,** Nr 10, 1194 (1960).
13. Besenbacher, F., Lægsgaard, E., Stensgaard, I., Stoltze, P., and Topsøe, H., *Catal. Lett.* **8,** 273 (1991).
14. Gay, J. G., and Richter, R., *J. Appl. Phys.* **61,** 3362 (1987).
15. Jonker, B. T., Walker, K. H., Kisker, E., Prinz, G. A., and Carbone, C., *Phys. Rev. Lett.* **57,** 142 (1986).

16. Koon, N. C., Jonker, B. T., Volkening, F. A., Krebs, J. J., and Prinz, G. A., *Phys. Rev. Lett.* **59,** 2463 (1987).
17. Strongin, D. R., Carrazza, J., Bare, S. R., and Somorjai, G. A., *J. Catal.* **103,** 213 (1987).
18. Ertl, G., Lee, S. B., and Weiss, M., *Surf. Sci.* **114,** 527 (1982).
19. Dumesic, J. A., Topsøe, H., and Boudart, M., *J. Catal.* **37,** 513 (1975).
20. Strongin, D. R., Bare, S. R., and Somorjai, G. A., *J. Catal.* **103,** 289 (1987).
21. Strongin, D. R., and Somorjai, G. A., *J. Catal.* **118,** 99 (1989).